

Altered Hepcidin Expression is Part of the Choroid Plexus Response to IL-6/Stat3 Signaling Pathway in Normal Aging Rats

Chongbin L^{1,2*}, Rui W¹, Chunyan W¹, Chen HU¹ and Qifeng D¹

¹Department of Physiology, Huzhou Teachers College, Huzhou, Zhejiang Province, P. R. China

²Zhejiang Provincial Key Lab for Technology and Application of Model Organisms, Wenzhou Medical University, Wenzhou, Zhejiang Province, P. R. China

Abstract

Accumulating evidence has revealed that brain iron concentrations increase with aging, and the choroid plexus may be at the basis of iron-mediated toxicity and the increase in inflammation and oxidative stress that occurs with aging. However, nothing is known concerning the correlation between the IL-6/Stat3 signaling pathway and the levels of hepcidin expression at the choroid plexus (CP) in normal aging. The morphological modifications as a function of aging were investigated and the present study used quantitative real time PCR (qPCR) and western blotting (WB) to determine the alterations in specific mRNA and corresponding protein changes at the CP on aging at ages 3, 6, 9, 12, 15, 18, 21, 24, 27, 30, 33 and 36 m Brown-Norway/Fischer (B-N/F) rats. Results showed that a striking deterioration of the CP epithelial cells, and results also firstly demonstrated that hepcidin expression at the choroid plexus increased with aging at the mRNA level and might cause corresponding changes in protein expression. These alterations in normal aging were in accordance with the expression and secretion of IL-6 and Stat3. Our data suggest that IL-6 regulate hepcidin expression at the choroid plexus, upon interaction with the cognate cellular receptor, and through the Stat3 signaling transduction pathway. The enhanced Stat3 signaling responsiveness to proinflammatory factors may impact on mechanisms of Alzheimer's disease.

Keywords: Aging; Choroid plexus; Hepcidin; IL-6; Stat3

Introduction

Advancing age is the major risk factor for many neurodegenerative disorders, including Alzheimer's disease (AD), a disease characterized by progressive memory and cognitive loss [1]. The predominant neuropathological hallmarks of AD are the accumulation of extracellular plaques containing insoluble amyloid- β (A β) peptide and intra-cellular neurofibrillary tangles [2]. Rapidly accumulating evidence indicates that nutritional iron enhances the neurotoxicity of A β and each of the major protein participants in AD pathology has physiologically important interactions with transition metals [3,4]. Clearance of A β from the brain occurs via active transport at the interfaces separating the central nervous system (CNS) from the peripheral circulation. The choroid plexus (CP), where the blood-cerebrospinal fluid barrier (BCSFB) is located, is a polarized tissue, with the basolateral side of the choroidal epithelium facing the blood and the apical microvilli in direct contact with the cerebrospinal fluid (CSF). The tissue plays a wide range of roles in brain development, aging, nutrient transport, endocrine regulation, and pathogenesis of certain neurodegenerative disorders [5-7]. Additionally, recent studies strongly suggest that increased levels of peripheral inflammation can induce a response in the CP and influence iron metabolism [8,9]. Taking this feature of the CP epithelial cells into account, it is plausible that the CP is functioning in the brain as a regulator of iron metabolism when an inflammatory environment is established. It would be of great interest to know if that is the case in normal aging, since it is recognized that the levels of pro-inflammatory cytokines in the blood increase with age [10,11], which can influence the secretion of iron-metabolism-related proteins, such as hepcidin (*Hamp*), by CP epithelial cells. A recent study has shown that increased peripheral markers of inflammation, measured in the blood of aged subjects, do not correlate with increased levels of blood circulating *Hamp* or low iron status in the brain [12]. However, nothing is known concerning the levels of *Hamp* in the brain cells or CSF of aged individuals. On the other hand, interleukin-6 (IL-6), which is able to trigger the cells signal transduction and activators

of transcription 3 (Stat3) signaling pathway appears to be associated with old-age anemia and is over-expressed in the aged mouse brain in response to lipopolysaccharide (LPS) [10]. Since IL-6 is shown to participate in the regulation of the expression of *Hamp*, not only in the liver [13] but also in the CP [9] of adult mice, it remains to be assessed if the CP contributes to the level of IL-6 in the aged brain. Moreover, the CP is able to up-regulate Stat3 gene in conditions of peripheral inflammation, and these may contribute to regional regulation of iron in the CNS [9]. In normal aging, however, the pattern of expression of this gene by the CP is still unknown. We propose to study the age-related alteration in IL-6/Stat3 pathway at the CP, which can elicit changes in the CP's capacity to regulate iron metabolism and to impact on the initiation and progression of brain pathology in AD.

Materials and Methods

Animals and tissue collection

All the procedures were performed in accordance with ethical guidelines on the care and use of animals in laboratory research which were approved by the Institutional Animal Ethics Committee (IAEC). Male Brown-Norway/Fischer (B-N/F) rats (n=96) were purchased from the Central Animal House of the College (Shanghai, China) on aging at ages 3, 6, 9, 12, 15, 18, 21, 24, 27, 30, 33 and 36 m. B-N/F rats are not as susceptible to cancer as the more inbred species and

*Corresponding author: Chongbin L, Department of Physiology, Huzhou Teachers College, Huzhou, Zhejiang Province 313000, P. R. China, Tel: 86-572-259-2572; Fax: 86-572-232-1203; E-mail: liuchongbin1972@126.com

Received February 20, 2014; Accepted April 25, 2014; Published April 28, 2014

Citation: Chongbin L, Rui W, Chunyan W, Chen HU, Qifeng D (2014) Altered Hepcidin Expression is Part of the Choroid Plexus Response to IL-6/Stat3 Signaling Pathway in Normal Aging Rats. Bioenergetics 3: 115. doi:[10.4172/2167-7662.1000115](https://doi.org/10.4172/2167-7662.1000115)

Copyright: © 2014 Chongbin L, et al. This is an open-access article distributed under the terms of the Creative Commons Attribution License, which permits unrestricted use, distribution, and reproduction in any medium, provided the original author and source are credited.

can live in excess of 36 m. Rats were anesthetized by intraperitoneal injection of pentobarbital (50 mg/kg), and then perfused with 0.9 M phosphate buffered saline (PBS), pH 7.4, at 4°C via the left ventricle of the heart, using a peristaltic pump (Harvard Apparatus, Holliston, MA, USA). The top of the cranium was removed and the two lateral ventricle CPs were then dissected out under a microscope to ascertain cell types present. Tissues were immediately transferred to an ice-cold microcentrifuge tube containing RNAlater (Ambion, Austin, TX, USA) to limit degradation by endonucleases and then stored at -80°C before quantitative real time PCR (qPCR) and western blotting (WB) analysis (All samples stored for an equal length of time before processing). For qPCR and WB, n = 8 (96 rats) were tested for each age group.

Electron microscopy

Samples of choroid plexus were fixed in 2.5% glutaraldehyde and 4% paraformaldehyde in 0.1 mol/L cacodylate buffer (pH 7.4). Specimens were post-fixed with 1% osmium tetroxide, dehydrated through ascending series of ethanol, and embedded in Epon. The serial semi-thin sections were stained with 1% toluidine blue and examined with a light microscope. The thin sections were viewed and photographed with a transmission electron microscope (Hitachi Ltd, Tokyo, Japan).

Quantitative real time PCR

Samples stored in RNA later were allowed to thaw and were rinsed with nuclease-free water before homogenizing in the lysis buffer provided in the Qiagen RNeasy kit (Qiagen, Valencia, CA, USA). This kit was used, according to the manufacturer's instructions, to extract the RNA. RNA concentrations were measured by a Nano Drop 1,000 spectrophotometer (Thermo Fisher Scientific, Wilmington, DE, USA) and stored at -80°C until further use. 1 µg of RNA was used with the Omniscript Reverse Transcription kit (Qiagen) to synthesize 20 µL of cDNA and then cDNA was used for real time reverse transcription quantitative PCR (qPCR). For qPCR, independent assays were performed using SYBR premix Ex Taq TM (Invitrogen, Carlsbad, CA, USA) with three biological replicates. Forward (F) and reverse (R) primers for each gene of interest were designed using Primer Premier software (PREMIER Biosoft International, Palo Alto, CA, USA). Primers used for the amplification of cDNA were summarized in Table 1. In each 25 µL quantitative real time reaction using SYBR-ER master mix, 10 mM primers and 1 µL cDNA were implemented. Reactions were run in a Bio-Rad iCycler system (Bio-Rad, Hercules, CA, USA) using Invitrogen's suggested protocol. The reactions were incubated at 72°C for 4 min, 4°C for 4 min, followed by a 30 cycles of 4 min at 94°C, 4 s at 94°C, 4 s at 56°C and 25 s at 72°C. Annealing temperatures (TA) varied and were specific for each primer set. The DNA band was visualized under UV light and was then extracted. The DNA was purified from each gel slice using Promega Wizard columns (Promega, Madison, WI, USA). All runs contained an inter run calibrator to account for any differences between runs. All data were normalized to the reference gene, β-actin, before statistical analysis was performed. The ΔΔCT method was used to calculate the normalized expression of each gene for each sample [14] and the specific band of interest gene was confirmed by DNA gel electrophoresis [15].

Western blotting analysis

Samples were washed and homogenized in RIPA buffer containing 1% Triton X-100. After centrifugation at 10,000 g for 30 minutes at 4°C, the supernatant was collected and protein concentration measured. Aliquots of the extract containing about 50 µg of protein were separated by reducing 15% SDS-PAGE and electro blotted onto PVDF

membranes for 45 min at room temperature. The membranes were blocked in 5% non-fat milk containing 20 mM Tris-HCl, pH 7.6, 137 mM NaCl, 0.1% Tween-20 (TBS-T) for 2 hours at room temperature, and then incubated with rabbit anti-mouse IL-6 (1: 5,000) (Alpha Diagnostic International) or rabbit anti-mouse phospho-stat3 (1: 2,000) (Santa Cruz Biotech) for overnight at 4°C. After washing with TBS-T three times, the membranes were incubated in anti-rabbit secondary antibody conjugated horseradish peroxidase (1: 5,000) (Amersham, UK) for 2 hours at room temperature. Immunoreactive proteins were detected by using the enhanced chemiluminescence method (ECL kit; Amersham), and quantified by transmittance densitometry using volume integration with Gel-Pro software. To ensure even loading of the samples, the same membrane was probed with rabbit anti-human β-actin antibody (1: 5,000) (Sigma-Aldrich, St. Louis, MO, USA). The intensity of the specific bands was detected and analyzed by Odyssey infrared imaging system (Li-Cor). IL-6 or phospho-stat3 protein levels in each specimen were normalized to β-actin.

Statistical analysis

For the qPCR analysis, Bio-Rad iQ5 Optical System software (Bio-Rad, Hercules, CA, USA) using the ΔΔCT method to calculate the normalized expression of each gene for each sample was employed [14]. Natural logarithm transformations of the data were used to correct for non-normality and inequality of variances, which was then confirmed by Shapiro-Wilk's and Levene's tests. Results were expressed as the mean ± standard deviation. A single-factor ANOVA followed by Tukey's pairwise comparisons were used to analyze the data. All statistical analyses were conducted using the SPSS 13.0 software (IBM, Armonk, NY, USA), and differences were assumed to be significant if the probability (P) value was < 0.05.

Results

The morphological modifications of the CP in normal aging rats

The senescence of the CP was a gradual aging process. Aged CP epithelial cells presented a general atrophy (Figure 1C) when compared to the adult CP (Figure 1A). The epithelial cells displayed a decrease in height, total volume and length of the apical microvilli (Figure 1F) when compared to the adult CP (Figure 1D). The basement membrane, stroma, and blood vessel walls of the CP became thicker with age (Figure 1B and 1C) when compared to the adult CP (Figure 1A). The tight junctions (TJ) of neighboring CP epithelial cells degenerated in aged rats (Figure 1G) when compared to the adult CP (Figure 1E). There was a massive and extensive fibrosis observed in the central stroma and the surrounding of the CP (Figure 1H), there were also responsible for the deficits in molecular exchanges between the CP and the CSF. Epithelial cells also acquired numerous lipofuscin vacuoles (Figure 1G) in normal aging animals. These modifications could alter choroid plexus functions, including synthesis, secretion and transport of proteins and other molecules.

cDNA	Sequence
IL-6	F: 5'- AGTTGCCTTCTTGGGACTGA-3' R: 5'- ACAGTGCATCATCGCTGTTTC-3'
Hecpidin	F: 5'- CTGCCTGTCTCCTGCTTCTC-3' R: 5'- GGAAGTTGGTGTCTCGCTTC-3'
P-Stat3	F: 5'- AGTTCTCGTCCACCACCAAG -3' R: 5'- CTAGCCAGACCAGAACGAG -3'
β-actin	F: 5'-CACGATGGAGGGGCCGGACTCATC-3' R: 5'-TAAAGACCTCTATGCCAACACAGT-3'

Table 1: Rat gene-specific PCR primers

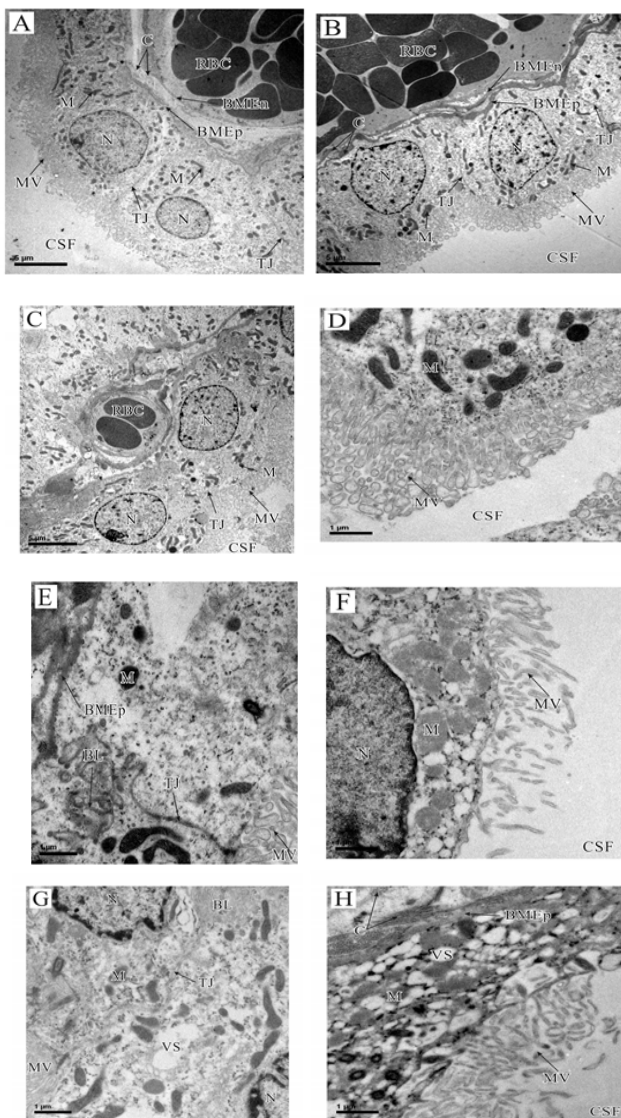


Figure 1: The morphological modifications of the CP in normal aging rats (A, D and E): components of adult rat lateral ventricle CP villus. Three epithelial cells comprise the apex of a villus projecting into CSF. Surfaces of epithelial cells are replete with microvilli (MV). Tight junctions (TJ) adjoin apical membranes of neighboring CP epithelial cells. Subjacent to epithelial cells is a sinusoidal blood vessel with several red cells (RBC). Clusters of collagen fibers (C) are seen in cross-section. Basement membranes (BMEp) lining the basal surfaces of CP epithelial cells are apparent as is the basement membrane (BME) of an endothelial cell lining the blood vessel. Numerous cytoplasmic organelles are visible in CP epithelial cells such as nuclei (N) and mitochondria (M). BL is the basal labyrinth. (B, C, F, G and H): The morphological modifications of the CP in aged CP epithelial cells. At the same time, epithelial cells acquire numerous vacuoles (VS) in aged rats.

The expression of hepcidin (*Hamp*) at the CP in normal aging rats

The expression of the *Hamp* at the messenger RNA (mRNA) level with age was measured by quantitative real time PCR. Results showed that there was a mild increase in *Hamp* expression from 3 to 18 m group, followed by a significant increase to 36 m group (Figure

2A). One-way ANOVA showed an effect of age for the twelve tested age groups at the $P < 0.05$ level [$F(11, 49) = 4.90, P = 0.021$]. Tukey's pairwise comparison revealed a significant difference in the mean natural log-transformed normalized expression of *Hamp* between 3 and 21 m, 3 and 24 m, 3 and 27 m, 3 and 30 m, 3 and 33 m, 3 and 36 m rats ($P < 0.05$, Figure 2B). However, the 3, 6, 9, 12, 15 and 18 m groups did not significantly differ from each other, or from 21 to 36 m groups (Figure 2B). Therefore, these results showed a continuous increase in the expression of *Hamp* at the CP epithelium after 21 m of age.

The mRNA and protein expression of interleukin-6 (IL-6) at the CP in normal aging rats

The expression of the IL-6 at the mRNA level as a function of aging was measured by quantitative real time PCR at 3, 6, 9, 12, 15, 18, 21, 24, 27, 30, 33 and 36 m groups. Results showed that there was a mild increase in IL-6 expression from 3 to 21 m group (except to 6 and 15 m groups), followed by a significant increase to 30 m and then a mild decrease to 36 m group (Figure 3A). A one-way ANOVA showed an effect of age for the twelve tested age groups at the $P < 0.05$ level [$F(11, 49) = 2.47, P = 0.047$]. Tukey's pair wise comparison revealed a significant difference in the mean natural log-transformed normalized expression of IL-6 between 6 and 24 m, 6 and 27 m, 6 and 30 m, 6 and 33 m, 6 and 36 m rats ($P < 0.05$, Figure 3B). However, the 3, 9, 12, 15, 18, and 21 m groups did not significantly differ from each other, or from 24 to 36 m groups (Figure 3B).

The protein expression of the IL-6 as a function of aging was also measured by western blotting. Results showed that there was a mild increase in IL-6 expression from 3 to 18 m group (except to 15 m group), followed by a significant increase to 33 m and then a mild decrease to 36 m group (Figure 4A). A one-way ANOVA showed an effect of age for the twelve tested age groups at the $P < 0.05$ level [$F(11, 49) = 3.08, P = 0.036$]. However, the 3, 6, 9, 12, 15, and 18 m groups did not significantly differ from each other, or from 21 to 36 m groups (Figure 4B). Therefore, CP IL-6 expression was either stable or increased with age.

The mRNA and protein expression of phosphorylated signal transduction and activators of transcription 3 (P-Stat3) at the CP in normal aging rats

The expression of the *P-Stat3* at the mRNA level with respect to age was measured by quantitative real time PCR. Results showed that there was an increase in *P-Stat3* expression from 3 to 36 m group (except to 6, 24, 27 and 33 m groups) (Figure 5A). A one-way ANOVA showed an effect of age for the twelve tested age groups at the $P < 0.05$ level [$F(11, 49) = 4.33, P = 0.037$]. Tukey's pair wise comparison indicated a significant difference in the mean natural log-transformed normalized expression of *P-Stat3* between 6 and 21 m, 6 and 30 m, 6 and 33 m, 6 and 36 m rats, and between 9 and 21 m, 9 and 30 m, 9 and 36 m rats ($P < 0.05$, Figure 5B). These results indicated that *P-Stat3* expression at the CP epithelium increased with age at the mRNA level. This effect became significant at 36 m.

The protein expression of the *P-Stat3* as a function of aging was also measured by western blotting. Results showed that there was a mild increase in *P-Stat3* expression from 3 to 21 m group (except to 9, 15, and 18 m groups), followed by a significant increase to 36 m group (except to 27 m group) (Figure 6A). A one-way ANOVA showed an effect of age for the twelve tested age groups at the $P < 0.05$ level [$F(11, 49) = 4.25, P = 0.028$]. However, the 3, 6, 9, 12, 15, and 18 m groups did not significantly differ from each other, or from 21 to 36 m groups (Figure 6B).

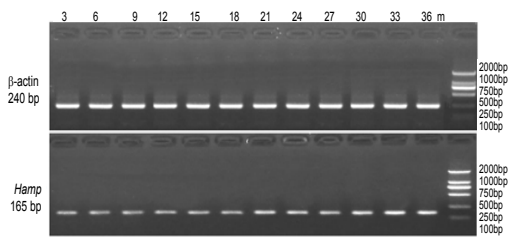


Figure 2A: Expression levels of hepcidin (Hamp) mRNA at the CP epithelium in normal aging rats

For real time reverse transcription quantitative PCR (qPCR), independent assays were performed using SYBR premix Ex Taq™ with three biological replicates. Gelred was added to the gel pre-run, the DNA band was visualized under UV light and was then extracted. It showed that there was a significant increase from 21 to 36 m group for the twelve aged groups, n = 8 for each age group.

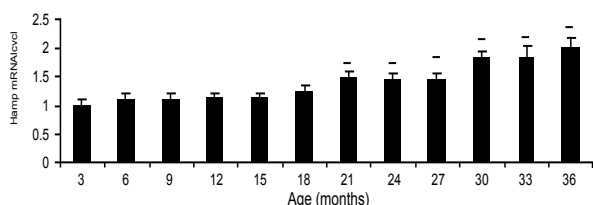


Figure 2B: The relative mRNA levels of hepcidin (Hamp) using real-time RT-PCR assay at the CP epithelium in normal aging rats.

The measured quantity of mRNA in each of treated samples was normalized using CT values obtained for the β-actin mRNA amplifications running in the same plate. The data were the means ± standard deviation of three sets of experiments.

Graph of the log-transformed normalized expression of Hamp with age, n = 8 for each age group tested. One-way ANOVA revealed an effect of age for the twelve tested age groups at the *P < 0.05 level.

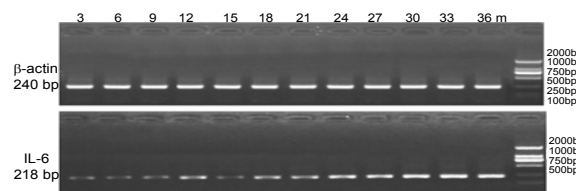


Figure 3A: mRNA expression levels of interleukin-6 (IL-6) at the CP epithelium in normal aging rats

For real time reverse transcription quantitative PCR (qPCR), independent assays were performed using SYBR premix Ex Taq™ with three biological replicates. Gelred was added to the gel pre-run, the DNA band was visualized under UV light and was then extracted. It showed that there was a significant increase from 24 to 30 m group for the twelve aged groups, n = 8 for each age group.

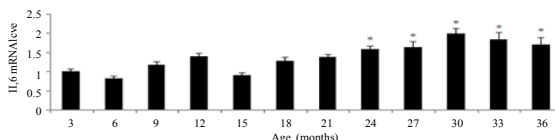


Figure 3B: The relative mRNA levels of interleukin-6 (IL-6) using real-time RT-PCR assay at the CP epithelium in normal aging rats

The measured quantity of mRNA in each of treated samples was normalized using CT values obtained for the β-actin mRNA amplifications running in the same plate. The data were the means ± standard deviation of three sets of experiments.

Graph of the log-transformed normalized expression of IL-6 with age, n = 8 for each age group tested. One-way ANOVA revealed an effect of age for the twelve tested age groups at the *P < 0.05 level.

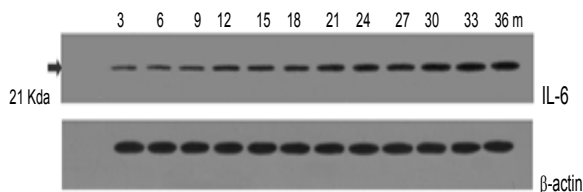


Figure 4A: Protein expression levels of interleukin-6 (IL-6) at the CP epithelium in normal aging rats

Immunoreactive proteins were detected by using the enhanced chemiluminescence method. It showed that there was a significant increase from 21 to 36 m group for the twelve aged groups, n = 8 for each age group.

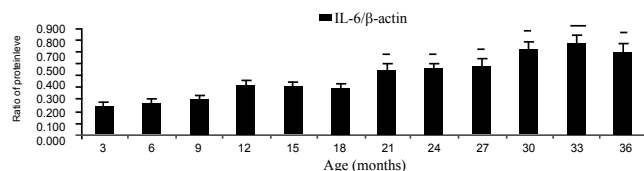


Figure 4B: The ratio of interleukin-6 (IL-6)/β-actin protein levels at the CP epithelium in normal aging rats

The intensity of the specific bands was detected and analyzed by Odyssey infrared imaging system. IL-6 protein levels in each specimen were normalized to β-actin.

Graph of the relative protein levels expression of IL-6 with age, n = 8 for each age group tested. One-way ANOVA revealed an effect of age for the twelve tested age groups at the *P < 0.05 and **P < 0.01 level.

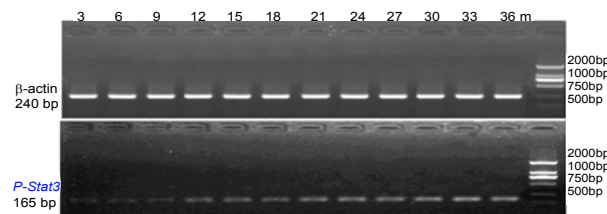


Figure 5A: mRNA expression levels of phosphorylated signal transduction and activators of transcription 3 (P-Stat3) at the CP epithelium in normal aging rats

For real time reverse transcription quantitative PCR (qPCR), independent assays were performed using SYBR premix Ex Taq™ with three biological replicates. Gelred was added to the gel pre-run, the DNA band was visualized under UV light and was then extracted. It showed that there was a significant increase from 3 to 36 m group for the twelve aged groups, n = 8 for each age group.

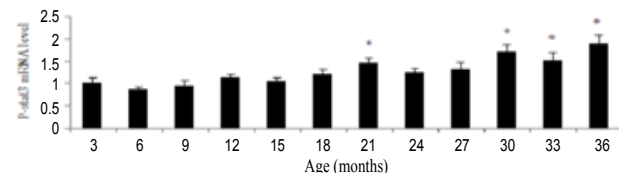


Figure 5B: The relative mRNA levels of phosphorylated signal transduction and activators of transcription 3 (P-Stat3) using real-time RT-PCR assay at the CP epithelium in normal aging rats

The measured quantity of mRNA in each of treated samples was normalized using CT values obtained for the β-actin mRNA amplifications running in the same plate. The data were the means ± standard deviation of three sets of experiments.

Graph of the log-transformed normalized expression of P-Stat3 with age, n = 8 for each age group tested. One-way ANOVA revealed an effect of age for the twelve tested age groups at the *P < 0.05 level.

Discussion

In this work, a striking deterioration of the CP epithelial cells is observed in aged rats (Figure 1). These modifications could alter choroid plexus functions, including synthesis, secretion and transport of proteins and other molecules. There are also responsible for the deficits in molecular exchanges between the CP and the CSF. It likely lead not only to abnormal brain A β clearance at the BCSFB, but also to the development of A β accumulation in this tissue. These results are in accordance with previous finding [3,16] in AD model rats.

In this study, in normal aging rats, we firstly found that there was a mild increase in *Hamp* expression at the CP from 3 to 18 m group rats, followed by a significant increase to 36 m group rats (Figure 2). Hepcidin is now regarded as the central regulator of body iron homeostasis [17,18]. Hepcidin also binds to the iron exporter Ferroportin-1 (FPN1), induces its internalization and degradation, and thereby blocks cellular iron efflux from neurons. Additionally, FPN1 is also found in the brain, mainly in the CP, in the ependymal cells lining the ventricles, and in neuromelanin cells in the substantia nigra [19]. In this study, we also found that there was a mild increase in IL-6 expression at the CP from 3 to 21 m group rats, followed by a significant increase to 30 m group rats (Figures 3 and 4). Silvestri, et al. [20] showed that the proximal 165 bp of the hepcidin promoter was critical for hepcidin activation in response to exogenously administered IL-6. High expression of the IL-6 may be involved in iron deprivation during infection and inflammation, through hepcidin induction and FPN1 down regulation. With advancing aging, microglia are activated to a reactive phenotype

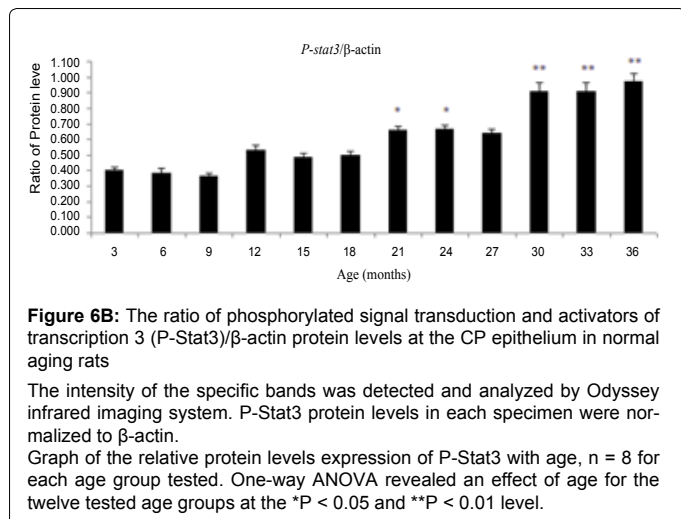
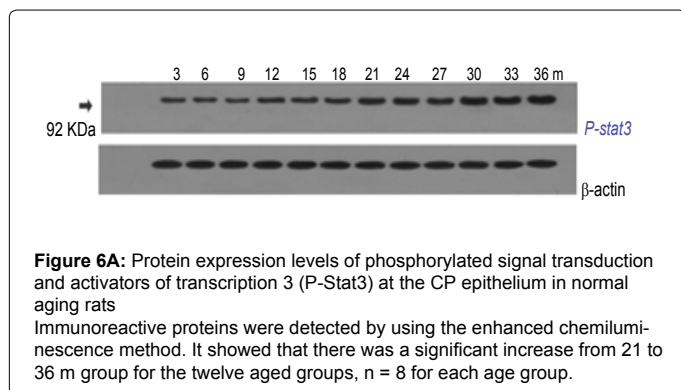
and release cytotoxic pro-inflammatory molecules including oxygen radicals, NO, glutamate, cytokines and prostaglandins, which can have a detrimental effect on other brain cells. In preliminary studies, it has shown that transferrin receptor 1 (Tfr1) and FPN1 were significantly downregulated in response to LPS treatment, while the divalent metal ion transporter (DMT1) and *Hamp* showed no change in expression under control conditions and after LPS treatment in N9 microglia cells [21]. This might suggest that iron homeostasis is under the control of alternative mechanisms in microglia, for instance cytokines such as IL-6. Whether iron accumulates in activated microglia (which could explain the association between increased iron stores and microglia activation in specific brain regions of AD) remains unknown. In this study, we firstly found that *P-Stat3* expression at the CP increased with age at the mRNA and protein levels (Figures 5 and 6). In normal aging, CP proteins will activate IL-6/Stat3 cell signal transduction pathway to alter transcriptin of *Hamp*, the gene which encodes hepcidin. In previous studies, it has shown that IL-6 regulated *Hamp* expression in the liver, upon interaction with the cognate cellular receptor, and through the Stat3 signaling transduction pathway [9,22-25]. We think that the same mechanism seems to be operational at the CP. Therefore, Stat3 is a key effector of baseline *Hamp* expression as well as during inflammatory conditions. Because the CP is composed not only of epithelial cells but also of a stroma containing endothelial cells of blood vessels and eventually immune cells, we next asked if epithelial cells of the CP were responsible for up-regulating the expression of genes encoding for *Hamp* and other iron-related genes.

Acknowledgments

The authors thank all reviewers and Prof. P.H. Backx (University of Toronto, Canada) and Prof. Z.M. Qian (The Hong Kong Polytechnic University, China) for critical reading. We are grateful to the Zhejiang Province Natural Sciences Foundation (Y2110388) and Zhejiang Province Technological Research (Y2011C37091) for financial support.

References

- Hardy J (2006) A hundred years of Alzheimer's disease research. *Neuron* 52: 3-13.
- Querfurth HW, LaFerla FM (2010) Alzheimer's disease. *N Engl J Med* 362: 329-344.
- Bush AI (2013) The metal theory of Alzheimer's disease. *J Alzheimers Dis* 33 Suppl 1: S277-281.
- Wang L, Xi G, Keep RF, Hua Y (2012) Iron enhances the neurotoxicity of amyloid β . *Transl Stroke Res* 3: 107-113.
- Mawuenyega KG, Sigurdson W, Ovod V, Munselli T, Kasten T, et al. (2010). Decreased clearance of CNS β -Amyloid in Alzheimer's disease. *Science* 330: 1774.
- Silverberg GD, Miller MC, Messier AA, Majmudar S, Machan JT, et al. (2010) Amyloid deposition and influx transporter expression at the blood-brain barrier increase in normal aging. *J Neuropathol Exp Neurol* 69: 98-108.
- Serot JM, Zmudka J, Jouanny P (2012) A possible role for CSF turnover and choroid plexus in the pathogenesis of late onset Alzheimer's disease. *J Alzheimers Dis* 30: 17-26.
- Marques F, Sousa JC, Correia-Neves M, Oliveira P, Sousa N, et al. (2007) The choroid plexus response to peripheral inflammatory stimulus. *Neuroscience* 144: 424-430.
- Marques F, Falcao AM, Sousa JC, Coppola G, Geschwind D, et al. (2009) Altered iron metabolism is part of the choroid plexus response to peripheral inflammation. *Endocrinology* 150: 2822-2828.
- Chen J, Buchanan JB, Sparkman NL, Godbout JP, Freund GG, et al. (2008) Neuroinflammation and disruption in working memory in aged mice after acute stimulation of the peripheral innate immune system. *Brain Behav Immun* 22: 301-311.
- Villeda SA, Luo J, Mosher KI, Zou B, Britschgi M, et al. (2011) The ageing



- systemic milieu negatively regulates neurogenesis and cognitive function. *Nature* 477: 90-94.
12. Ferrucci L, Semba RD, Guralnik JM, Ershler WB, Bandinelli S, et al. (2010) Proinflammatory state, hepcidin, and anemia in older persons. *Blood* 115: 3810-3816.
 13. Lee P, Peng H, Gelbart T, Wang L, Beutler E (2005) Regulation of hepcidin transcription by interleukin-1 and interleukin-6. *Proc Natl Acad Sci U S A* 102: 1906-1910.
 14. Schmittgen TD, Livak KJ (2008) Analyzing real-time PCR data by the comparative C(T) method. *Nat Protoc* 3: 1101-1108.
 15. Ke Y, Chen YY, Chang YZ, Duan XL, Ho KP, et al. (2003) Post-transcriptional expression of DMT1 in the heart of rat. *J Cell Physiol* 196: 124-130.
 16. Johansson PA, Dziegielewska KM, Liddel SA, Saunders NR (2008) The blood-CSF barrier explained: when development is not immaturity. *Bioessays* 30: 237-248.
 17. Darshan D, Anderson GJ (2009) Interacting signals in the control of hepcidin expression. *Biomaterials* 22: 77-87.
 18. Ganz T, Nemeth E (2011) Heparin and disorders of iron metabolism. *Annu Rev Med* 62: 347-360.
 19. Clardy SL, Wang X, Boyer PJ, Earley CJ, Allen RP, et al. (2006) Is ferroportin-hepcidin signaling altered in restless legs syndrome? *J Neurol Sci* 247: 173-179.
 20. Silvestri L, Pagani A, Camaschella C (2008) Furin-mediated release of soluble hepcidin: a new link between hypoxia and iron homeostasis. *Blood* 111: 924-931.
 21. Ward RJ, Crichton RR, Taylor DL, Della Corte L, Srani SK, et al. (2011) Iron and the immune system. *J Neural Transm* 118: 315-328.
 22. Stoian I, Manolescu B, Atanasiu V, Lupescu O, BuÅŸu C (2007) IL-6 - STAT-3 - hepcidin: linking inflammation to the iron metabolism. *Rom J Intern Med* 45: 305-309.
 23. Sakamori R, Takehara T, Tatsumi T, Shigekawa M, Hikita H, et al. (2010) STAT3 signaling within hepatocytes is required for anemia of inflammation in vivo. *J Gastroenterol* 45: 244-248.
 24. Armitage AE, Eddowes LA, Gileadi U, Cole S, Spottiswoode N, et al. (2011) Heparin regulation by innate immune and infectious stimuli. *Blood* 118: 4129-4139.
 25. Pagani A, Nai A, Corna G, Bosurgi L, Rovere-Querini P, et al. (2011) Low hepcidin accounts for the proinflammatory status associated with iron deficiency. *Blood* 118: 736-746.